Characterization of human lysophospholipid acyltransferase 3[S]

Shilpa Jain,* Xiaoling Zhang,† Preeti J. Khandelwal,* Aleister J. Saunders,* Brian S. Cummings,† and Peter Oelkers[1,*]

Department of Biology,* Drexel University, Philadelphia, PA, 19104; and Department of Pharmaceutical and Biomedical Sciences,† University of Georgia, Athens, GA 30602

Abstract **Esterifying lysophospholipids may serve a variety of functions, including phospholipid remodeling and limiting the abundance of bioactive lipids. Recently, a yeast enzyme, Lpt1p, that esterifies an array of lysophospholipids was identified. Described here is the characterization of a human homolog of *LPT1* that we have called lysophosphatidylcholine acyltransferase 3 (LPCAT3). Expression of LPCAT3 in Sf9 insect cells conferred robust esterification of lysophosphatidylcholine in vitro. Kinetic analysis found apparent cooperativity with a saturated acyl-CoA having the lowest $K_{0.5}$ (5 μM), a monounsaturated acyl-CoA having the highest apparent V_{max} (759 nmol/min/mg), and two polyunsaturated acyl-CoAs showing intermediate values. Lysophosphatidylethanolamine and lysophosphatidylserine were also utilized as substrates. Electrospray ionization mass spectrometric analysis of phospholipids in Sf9 cells expressing LPCAT3 showed a relative increase in phosphatidylcholine containing saturated acyl chains and a decrease in phosphatidylcholine containing unsaturated acyl chains. Targeted reduction of LPCAT3 expression in HEK293 cells had essentially an opposite effect, resulting in decreased abundance of saturated phospholipid species and more unsaturated species. Reduced LPCAT3 expression resulted in more apoptosis and distinctly fewer lamellipodia, suggesting a necessary role for lysophospholipid esterification in maintaining cellular function and structure.**—Jain, S., X. Zhang, P. J. Khandelwal, A. J. Saunders, B. S. Cummings, and P. Oelkers. **Characterization of human lysophospholipid acyltransferase 3. *J. Lipid Res.* 2009.** 50: **1563–1570.**

Supplementary key words acyl-CoA • apoptosis • lamellipodia • mass spectrometry • membrane composition • substrate specificity

Lysophospholipids (lysoPLs[2], monoacylglyercophospholipids) may be esterified for several physiological reasons. One is the intracellular remodeling of glycerophospholipids (PL). Pairing phospholipase A_2 activity with lysoPL esterification allows for the alteration of PL acyl-chain composition (Lands Cycle) (1). Acyl chain composition of PL may impact cellular membrane dynamics (2) and influence cellular processes such as endocytosis (3). The predominance of palmitoyl chains in surfactant phospholipids (4) and linoleoyl chains in mitochondrial cardiolipin (5) underscores the need for modifying acyl chain composition after de novo phospholipid synthesis. Selective incorporation of arachidonyl chains into the sn-2 position also allows for the priming of phospholipase A_2 initiated signal cascades (6). Another physiological reason to esterify lysoPL, especially lysophosphatidylcholine (lysoPC), is to limit signaling through G-protein coupled receptors (7).

How cells esterify lysoPL has recently begun to be elucidated. Acyl-CoA independent, transacylation can be mediated by the mitochondrial tafazzin (5). Acyl-CoA dependent esterification of lysoPC, lysophosphatidic acid (lysoPA), and lysophosphatidylglycerol (lysoPG) can be mediated in the endoplasmic reticulum (ER) by lysophosphatidylcholine acyltransferase 1 (LPCAT1) (8, 9). Saturated acyl-CoA substrates are used preferentially but not exclusively. LPCAT2 is 48% identical to LPCAT1, localizes to the ER and Golgi, has a broader pattern of tissue expression, and only uses lysoPC as an acyl acceptor (10). Among the lysoPC

This work was supported by funding from the Department of Bioscience and Biotechnology, Drexel University (P.O.) and a Georgia Cancer Coalition Distinguished Scholar and University of Georgia Junior Faculty grant (B.S.C.).

Manuscript received 29 July 2008 and in revised form 27 February 2009 and in re-revised form 7 April 2009.

Published, JLR Papers in Press, April 7, 2009.
DOI 10.1194/jlr.M800398-JLR200

Abbreviations: AGPAT, 1-acyl-sn-glycerol-3-phosphate acyltransferase; ATYL, acyl-transferase-like; DGAT, diacylglycerol acyltransferase; ESI-MS, electrospray ionization–mass spectrometry; HEK, human embryonic kidney; LPCAT, lysophosphatidylcholine acyltransferase; LPLAT, lysophospholipid acyltransferase; MBOAT, membrane bound o-acyltransferase; MOI, multiplicity of infection; MTT, 3-(4, dimethylthiazolyl-2)-2, 5-diphenyltetrazolium bromide; NS, non-silencing; PA, phosphatidic acid; PAF, platelet activating factor; PC phosphatidylcholine; ePC, 1-alkyl 2-acyl phosphatidylcholine; PE, phosphatidylethanolamine; PG, phosphatidylglycerol; PI, phosphatidylinositol; PI, propidium iodine; PL, glycerophospholipid; PS, phosphatidylserine.

[1]To whom correspondence should be addressed.
e-mail: oelkersp@arcadia.edu

[S]The online version of this article (available at http://www.jlr.org) contains supplementary data in the form of four figures.

species utilized is 1-alkyl lysoPC and 1-alkenyl lysoPC, indicating the likely importance of this enzyme in platelet activating factor (PAF) synthesis. A third mouse paralog can also esterify lysoPC with a preference for palmitoyl-CoA (11).

The *S. cerevisiae* genome contains no gene with distinct sequence identity to these mouse LPCAT. However, an unrelated gene, *LPT1* (also called *ALE1*, *LPA1*, and *SLC4*) encodes for a lysoPL acyltransferase (LPLAT) (12–16). Lpt1p can esterify all the lyso species of the major phospholipids, has highest capacity for unsaturated acyl-CoA species, and belongs to the membrane bound o-acyltransferase (MBOAT) gene family (17) which has many representatives in mammalian genomes. Pioneering work by Hishikawa et al. (18) identified and characterized three mouse MBOAT paralogs, LPCAT3, LPCAT4, and LPEAT1, that can esterify lysoPC, lysoPE and/or lysoPS. Zhou et al. (19) have shown that human LPCAT3 esterified lysoPC and lysoPS in vitro and that reduction of its expression in Huh7 cells dramatically reduced LPCAT activity.

We have performed similar kinetic analyses of human LPCAT3, with some different results. We have used mass spectrometry to analyze the effect of LPCAT3 overexpression and reduced expression on phospholipid composition. Data are also provided that support a role for LPCAT3 in regulating cell growth and apoptosis.

MATERIALS AND METHODS

Materials

Lysophosphatidylethanolamine (lysoPE), lysophosphatidylserine (lysoPS), lysophosphatidylinositol (lysoPI), 1-O-alkyl lysoPC, and lysoPG were from Avanti Polar Lipids (Alabaster, AL). [1-^{14}C] palmitoyl- lysoPC (55mCi/mmol) was from Perkin-Elmer Life. All other chemicals were obtained from Sigma or Fisher.

Methods

Protein sequence analysis. Full-length sequences were aligned using clustalW2 (20). For percent identity, the conserved amino acids were counted and divided by the length of the shorter of the two proteins compared. Transmembrane domains were predicted by the TMHMM2.0 program (21).

Insect cell expression. A 4.4 kb human LPCAT3 cDNA clone (GenBank Acc. #BC065194) was obtained from the American Type Culture Collection in pCMVsport6. Restriction digest with *SmaI*, *PvuII* released the open reading frame with 45 bp of 5′UTR and 121 bp of 3′UTR. This fragment was ligated into *StuI* digested pFastbac and sequenced. Subsequent baculovirus expression in Sf9 insect cells was performed in the Wistar Institute Protein Expression Core Facility. The pFastbac/LPCAT3 plasmid and a pFastbac/Glutathione S-transferase (GST) control were transposed into DH10Bac cells. Recovered bacmid DNA was screened by PCR for proper transposition of the transfer vector into the baculovirus genome. Positive bacmid DNA was transfected into Sf9 cells, and passage 1 (P1) virus stocks were recovered 96 h. posttransfection. A high-titer P2 virus stock was generated by infecting Sf9 at a multiplicity of infection (MOI) of ~0.1, followed by incubation for 96–120 h. For production, 1×10^6 Sf9 cells/ml in Sf900-II medium (Invitrogen) at 28°C were infected with viruses at an MOI of 1. Cells were harvested 48 h postinfection.

Generating cell lysates for enzymatic assays. Sf9 cells were homogenized in 1 mM EDTA / 200 mM sucrose / 100 mM Tris-HCl, pH 7.4 by 10–15 passages through a 26.5 gauge needle (22). Unlysed cells were removed by centrifugation at 1,000 *g* for 5 min at 4°C. The supernatant was stored frozen (−70°C) prior to assays.

LPCAT assay, radioactive substrate. Lysophosphatidylcholine acyltransferase (LPCAT) activity was measured by the incorporation of [1-^{14}C]palmitoyl lysoPC into phosphatidylcholine (PC). The reaction contained 100 mM Tris-HCl, pH 7.4, 50 μM [1-^{14}C] palmitoyl lysoPC (50,000 dpm/nmol), 1–150 μM of the respective acyl-CoA, and 1 μg of cell lysate protein in a total volume of 100 μl. Fixed time assays were performed for 7.5 min at 28°C or 5 min at 37°C. Reactions were stopped by adding chloroform: methanol (2:1) and lipids were extracted, resolved by thin layer chromatography, and quantified as described elsewhere (8). EZ-Fit software was used for Hill-Plots. To calculate V_{max}/K_m, V_{max} was first changed to nM/min/mg to remove volume from the units of the ratio.

LPLAT assays, spectrophotometry. These assays were essentially performed as described previously (13). The reaction mixture contained 100 mM Tris-HCl, pH 7.4, 50 μM of the respective lysoPL, 50 μM oleoyl CoA, 1 mM dithionitrobenzoic acid (DTNB), and 2–5 μg cell lysate protein in a total volume of 1 ml. Real time assays were performed for 5 min at room temperature or 3 min at 37°C.

Bligh-Dyer lipid extraction. Cellular PL was extracted using chloroform and methanol according to the method of Bligh and Dyer (23). Following transfection, Sf9 cells were homogenized in 3 ml of methanol: water (2:0.8), transferred to a glass test tube, and then 1.25 ml chloroform was added. Tubes were vortexed for 30 s and allowed to sit for 10 min on ice. After centrifugation at 213 *g* for 1 min, the chloroform layer was collected. The extraction was repeated and lipid extracts combined, dried under argon, reconstituted with 50 μl of methanol:chloroform (2:1), and stored at −20°C.

Lipid phosphorus assay. Lipid phosphorus was quantified using malachite green (22). 10 μl of lipid extract was dried under argon. 200 μl of perchloric acid was added and heated at 130°C for 2–3 h. To this was added 1 ml of dH_2O, 1.5 ml of reagent C (4.2 g ammonium molybdate tetrahydrate in 100 ml 5 N HCl and 0.15 g malachite green oxalate in 300 ml dH_20), and 200 μl of 1.5% (v/v) Tween 20. After 25 min at room temperature, the A_{590} was measured.

Electrospray ionization–mass spectrometry (ESI-MS). Lipid extracts (500 pmol/μl) were prepared by reconstituting in chloroform: methanol (2:1). Mass spectrometry was performed as described previously (24). Samples were analyzed using a Trap XCT ion-trap mass spectrometer (Agilent Technologies, Santa Clara, CA) equipped with an ESI source. 5 μl of sample was introduced by means of a flow injector into the ESI source at a rate of 0.2 ml/min. The elution solvent was acetonitrile:methanol:water (2:3:1, v/v/v) containing 0.1% (w/v) ammonium formate (pH 6.4). The mass spectrometer was operated in the positive and negative ionization modes with a nitrogen drying gas flow-rate of 8.0 L/min at 350°C, nebulizer pressure at 30 psi, and capillary voltage at 3 kV. As previously described (24), qualitative identification of individual PL molecular species was based on their calculated theoretical monoisotopic mass values and subsequent

MS^n fragmentation to identify the polar head groups. Relative quantification was done by comparison to the most abundant phospholipid in each sample, which corresponded to *m/z* 760 or 34:1 (16:0, 18:1) PC. MassLynx 4.0 software was used for data analysis. MS^n fragmentation was performed on the same instrument under similar conditions except that the ion source and ion optic parameters were optimized with respect to the positive molecular ion of interest. Data from four separate Sf9 infections underwent ANOVA using SAS software. Individual means were compared using Student's *t*-test.

Transfection of HEK293 cells. HEK293 (human embryonic kidney) cells were seeded in 24 well plates at a concentration of 2.5×10^5 cells/well (~30% confluence) and allowed to grow for 24 h prior to transfection. 1 μg of pSM2 either encoding for a short hairpin RNA (shRNA) specific for LPCAT3 (Open Biosystems clone #V2HS 200012) or for a nonsilencing (NS) control (with a target sequence not complementary to any known human gene) was gently mixed with 1 μl of lipofectamine transfection reagent (InVitrogen Life Sciences) in 100 μl of Opti-MEM I reduced-serum medium (Life Sciences). After 20 min at room temperature, the mixtures were added drop-wise onto the cells. Subsequent experimentation was done after culturing in serum-free DMEM at 37°C for 24 h.

Analyses of cell metabolism, abundance, and viability. Activity of Complex I of the electron transport chain was determined by adding 30 μl of 5 mg/ml MTT (3-(4, dimethylthiazolyl-2)-2, 5-diphenyltetrazolium bromide) to each well. After 2 h incubation at 37°C, the media was replaced with 800 μl of DMSO to dissolve the resulting purple formazan, and the absorbance at 544 nm was measured with a FLUOstar OPTIMA plate reader (BMG Labtechnologies, Inc., Durham, NC). Cell number and viability were assessed using the ViaCount® assay reagent on EasyCyte Mini Guava flow cytometer (Guava Technologies, Hayward, CA) according to the manufacturer's instructions. Briefly, 25 μl cell suspensions were combined with 450 μl of assay reagent containing 7-Amino-actinomycin D (7-AAD) and propidium iodide (PI). Following 5 min incubation, cell number and viability were assessed by alterations in both 7-AAD and PI staining as well as alterations in forward scatter.

Assessment of apoptosis. Apoptosis and necrosis were assessed using annexin V (apoptotic cell marker) and propidium iodide (PI, necrotic cell marker) staining and flow cytometry as previously described (25) with modifications. Cisplatin (50 μM) and tert-butylhydroperoxide (500 μM) were used as positive controls for apoptosis and necrosis, respectively. Following treatment, media were removed, cells washed twice with PBS and incubated in binding buffer (10 mM HEPES, 140 mM NaCl, 5 mM KCl, 1 mM $MgCl_2$, 1.8 mM $CaCl_2$, pH = 7.4) containing annexin V-FITC (25 μg/ml) and PI (25 μg/ml) for 10 min. Cells were washed three times using binding buffer, released from the monolayers using a rubber policeman and staining quantified using a Becton Dickinson FacsCalibur flow cytometer. For each measurement, 10,000 events were counted.

Assessment of cell morphology. Cell morphology was determined using phase-contrast microscopy as previously described (25, 26) with modifications. Briefly, cells were washed twice with PBS, fixed for 20 min using 10% buffered formalin, 4% formaldehyde, washed with PBS, covered with mounting media (Sigma), and cover slips applied. Visualization was performed using a TE300 Eclipse microscope (Nikon, Melville, NY).

RESULTS

Identification of human MBOAT5 as a LPT1 homolog

Using the yeast Lpt1p amino acid sequence as the query, a blastp search (27) identified three human proteins with about 25% identity. These likely paralogs were originally identified as MBOAT 1, 2, and 5 with conservation of a putative acyltransferase domain (Pfam PFO3062) (17). MBOAT5 was chosen for initial analysis because, like Lpt1, it contains a C-terminal ER retention signal, KKXX (28). Subsequent studies have renamed human MBOAT5 as LPCAT3 (19, 29, 30). The predicted protein has 487 amino acids, a molecular weight of 56 kDa, and seven algorithm-identified (21) transmembrane domains.

Biochemical characterization of LPCAT3

A putative full-length cDNA clone for LPCAT3 was found in the mammalian gene collection (31) and inserted into baculovirus. This virus was used to drive expression in Sf9 insect cells. Precedents indicated that Sf9 cells harbor low levels of endogenous acyltransferase activity in general (22, 32). Parallel infection with a GST-encoding virus allowed for the measurement of endogenous activity. In vitro LPCAT assays at 28°C found LPCAT3 expression to confer 10-fold higher activity than GST-expression (**Fig. 1**). This temperature was primarily used for subsequent assays as it yielded 5-fold more activity than parallel assays at the physiological temperature of 37°C (Fig. 1).

To kinetically characterize the substrate specificity of LPCAT3, acyl-CoA concentration series assays were performed with four qualitatively different species. These represent the main classes of long chain acyl-CoAs: saturated (stearoyl-CoA); monounsaturated (oleoyl-CoA); polyunsaturated, omega-6 (arachidonic acid); and polyunsaturated, omega-3 (α-linolenoyl-CoA). Since the oleoyl-CoA curve was visibly sigmoidal (**Fig. 2**), suggesting cooperativity, Hill plots of all kinetic data were generated (see supplementary Figs. I and II). Cooperativity was found in all cases except linolenyl-CoA at 28°C. These same plots were

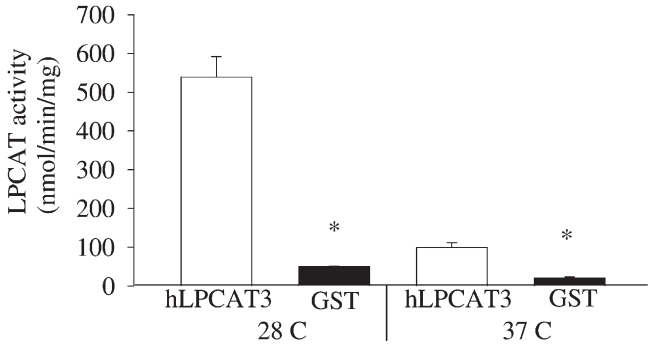

Fig. 1. LPCAT activity in infected Sf9 insect cells. Cell lysates from Sf9 cells with baculovirus-mediated expression of LPCAT3 or GST were assayed for LPCAT activity. 50 μM [1-^{14}C] palmitoyl-lysoPC, 50 μM oleoyl-CoA, 1 μg cell lysate, and 100 mM Tris-HCl, pH 7.4 were incubated for 7.5 min. at 28°C or 5 min. at 37°C. Radioactive product (PC) was resolved from substrate (lysoPC) by TLC. The data represent mean ± SE; n = 4. GST, glutathione S-transferase; LPCAT, lysophosphatidylcholine acyltransferase.

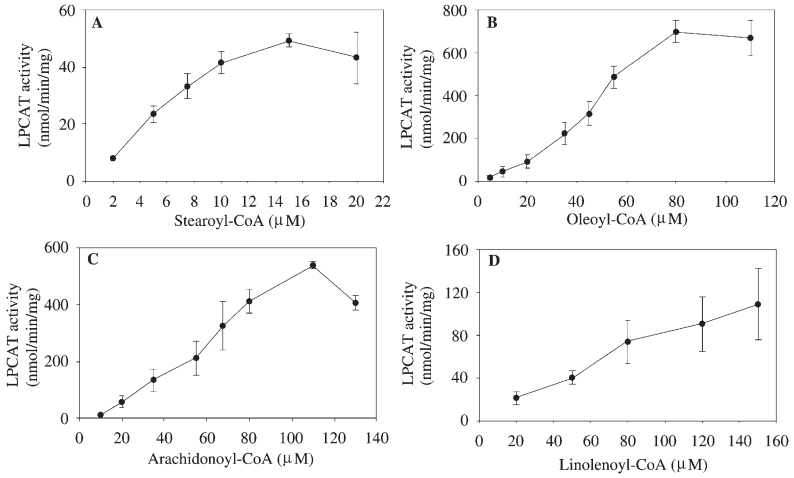

Fig. 2. Acyl-CoA substrate specificity of LPCAT3. LPCAT assays were performed as described in Fig. 1 except a range (1–150 μM) of each acyl-CoA was used. A: Stearoyl-CoA. B: Oleoyl-CoA. C: Arachidonyl-CoA. D: α-linolenoyl-CoA. For each data point, net LPCAT activity was obtained by subtracting LPCAT activity in Sf9-GST lysates from Sf9-LPCAT3 lysates. The data represent mean ± SE; n = 4. Data from parallel assays at 37°C are shown in supplementary Fig. II. GST, glutathione S-transferase; LPCAT, lysophosphatidylcholine acyltransferase.

used to determine the $K_{0.5}$ and apparent V_{max} values (**Table 1**). In terms of affinity ($K_{0.5}$), the substrate preference was stearoyl-CoA > oleoyl-CoA ⩾ arachidonyl-CoA ⩾ α-linolenoyl-CoA. Arachidonyl-CoA showed higher affinity at 28°C than at 37°C. In terms of capacity (V_{max}), oleoyl-CoA had the highest at 28°C and linolenoyl-CoA at 37°C. Because all of the reactions have the same, although undetermined, enzyme concentration, $V_{max}/K_{0.5}$ should be proportional to the catalytic efficiency (k_{cat}/K_m). This value was the highest for oleoyl-CoA. Clearly, the degree and placement of double bonds within the acyl-CoA substrate affects utilization by LPCAT3. α-Linolenoyl-CoA was the only substrate for which concentrations above 110 μM did not inhibit activity.

The kinetics of LPCAT3 were further analyzed by performing a lysoPC substrate concentration series with oleoyl-CoA as the acyl donor (**Fig. 3**). Again, cooperativity was observed with a Hill plot showing a Hill number of 1.7, $K_{0.5}$ of 13.1 μM, and an apparent V_{max} of 486 nmol/min/mg. Since oleoyl-CoA was kept at 50 μM, a value that turned out to be less than saturating, the V_{max} was less than that observed for oleoyl-CoA. Further analysis was performed with a single concentration (50 μM) of lysoPC species with varying sn-1 acyl chains (**Fig. 4**). Neither length nor degree of saturation affected utilization. However, the ether linkage in 1-alkyl lysoPC abrogated activity (data not shown). Varying the head group on the lysoPL also had a distinct effect on activity. Comparing 14:0 lysoPE to 14:0 lysoPC and 18:1 lysoPS to 18:1 lysoPC shows a 7-fold preference for lysoPC (Fig. 4). However, other species of lysoPE and lysoPS may be utilized to a greater degree. Esterification of lysophosphatidic acid (lysoPA), lysoPG, and lysoPI was assayed for but not detected (data not shown). This was also the case for lysoPS at 37°C (see supplementary Fig. IV). The structural features common to the acyl-acceptors utilized by LPCAT3 are an amine in the head group and a sn-1 acyl group attached through an ester linkage.

Effect of expressing LPCAT3 on phospholipid species in Sf9 cells

To begin to examine the physiological role of LPCAT3 in PL metabolism, the effect of expressing LPCAT3 on the PL profile in Sf9 cells was measured. ESI-MS was performed on four independently generated cell lysates expressing LPCAT3 and GST. To account for alteration in ionization efficiency, the relative abundance of each PL species was expressed relative to the most abundant species (34:1 PC; *m/z* 760) within the sample. Normalizing to an added standard (28:0 PC, *m/z* 678) was also performed and showed similar trends (data not shown). After analyzing the abundance of 73 different *m/z* values in the positive mode, 10 showed a significant difference between the LPCAT3 and GST expressing cells. Assigning specific PL species to *m/z* values was based on their calculated theoretical monoisotopic masses and verified by MS-MS. The five species that increased with LPCAT3 expression were 32:0 PE, 32:0 PC, 36:0 PC, 32:0 (1-alkyl) PC, and 34:1 (1-alkyl)

TABLE 1. Kinetic parameters of human LPCAT3

Acyl-CoA	Temp °C	$K_{0.5}$ μM	Apparent V_{max} nmol/min/mg	V_{max} / $K_{0.5}$ min^{-1} mg^{-1}	Hill number
stearoyl-CoA (18:0)	28	5.1	50	9.8	2.7
oleoyl-CoA (18:1)	28	46.5	759	16.3	2.0
arachidonyl-CoA (20:4)	28	55.8	529	9.5	2.0
α-linolenoyl-CoA (18:3)	28	214.0	268	1.3	1.0
stearoyl-CoA (18:0)	37	2.1	6	2.6	3.7
oleoyl-CoA (18:1)	37	12.2	87	7.1	1.6
arachidonyl-CoA (20:4)	37	245.0	82	0.3	2.0
α-linolenoyl-CoA (18:3)	37	232.0	323	1.4	1.4

Kinetic data from Fig. 2 and supplementary Fig. II were used to calculate $K_{0.5}$ and apparent V_{max} using Hill plots (see supplementary Figs. I and III). LPCAT, lysophosphatidylcholine acyltransferase.

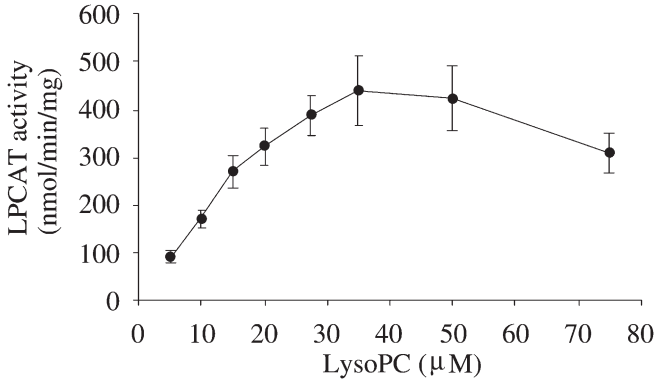

Fig. 3. Kinetics of lysoPC utilization by LPCAT3. LPCAT assays were performed as described in Fig. 1 except a range (5–75 μM) of [1-^{14}C] palmitoyl lysoPC was used. The data represent the mean of the net LPCAT activity ± SE; n = 4. LPCAT, lysophosphatidylcholine acyltransferase.

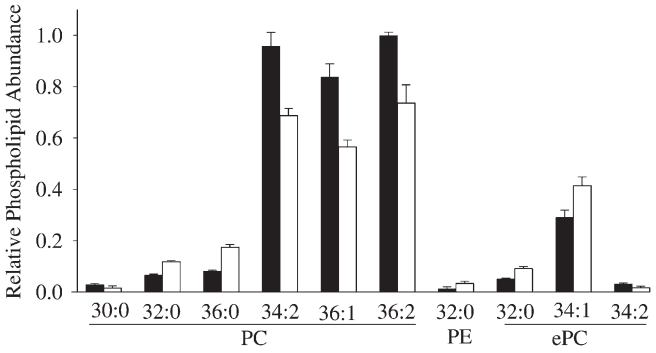

Fig. 5. Affect of LPCAT3 expression on Sf9 phospholipid species. Lipids were isolated from Sf9 cells expressing GST (dark bars) or LPCAT3 (light bars). After lipid phosphorous content determination, 250 nmol was analyzed by ESI-MS as described in Materials and Methods. The results from four independent Sf9 infections were averaged. The abundance of each PL species is expressed relative to that of the most abundant within the sample (34:1 PC in each case). Of the 73 *m/z* values analyzed, all the ones that statistically differed between GST and LPCAT3 are shown; $P < 0.05$. Standard error bars are shown. ePC = 1-alkyl 2-acyl phosphatidylcholine. GST, glutathione S-transferase; LPCAT, lysophosphatidylcholine acyltransferase.

PC. The five species that decreased were 30:0 PC, 34:2 PC, 36:1 PC, 36:2 PC, and 34:2 (1-alkyl) PC (**Fig. 5**). The overall trend was that the abundance of PC with more saturated chains increased with LPCAT3 expression whereas PC with more unsaturated chains became less abundant. One thing to note is that when normalized to the added standard, 34:1 PC was about 30% more abundant in the LPCAT3 expressing cells. No differences between LPCAT3 and GST expressing cells were detected in the negative mode, suggesting that PI and PS species were unaffected.

Cellular effects of reducing LPCAT3 expression in HEK293 cells

The converse experiment was then performed by reducing LPCAT3 expression in HEK293 cells by transfection with specific shRNA. The 21 nucleotide target is in a section of LPCAT3 that shares no homology with LPCAT4 or LPEAT1. Reduced LPCAT3 expression was confirmed by RT-PCR due to the lack of a commercially available antibody and resulted in significant changes in phospholipid species (**Figs. 6, 7A**). The trend was greater incorporation of long, polyunsaturated acyl chains into phospholipids when LPCAT3 expression is reduced. There was a concomitant decrease in free arachidonic (20:4) and linoleic (18:2) acid. These changes in phospholipid and fatty acid abundance coincided with a 30% reduction in cell number (Fig. 7B). MTT staining, a measure of cellular redox state, was similarly reduced by 30% (Fig. 7C), consistent with the reduction in cell number.

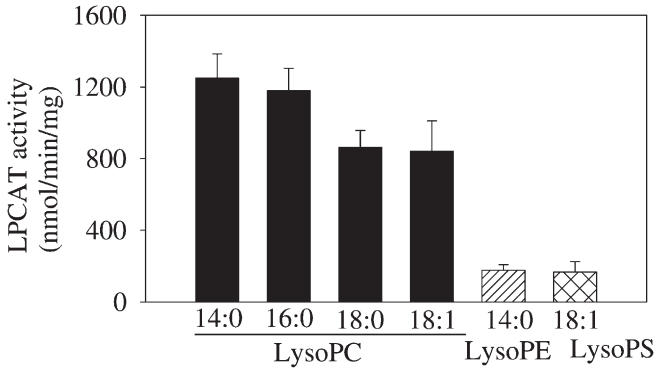

Fig. 4. LysoPL substrate specificity of LPCAT3. LPLAT activity was measured using 50 μM oleoyl-CoA and 50 μM of lysoPC (1-myristoyl (C14:0), 1-palmitoyl (C16:0), 1-stearoyl (C18:0), 1-oleoyl (C18:1)), 1-myristoyl (14:0) lysoPE, and 1-oleoyl (18:1) lysoPS at 28°C. The spectrophotometric method was used, as described in Materials and Methods, with lysates prepared from LPCAT3 or GST expressing Sf9 cells. The data represents mean ± SE; n = 4. Data from parallel assays at 37°C are shown in supplementary Fig. IV. GST, glutathione S-transferase; LPCAT, lysophosphatidylcholine acyltransferase.

To further examine the effect of reduced LPCAT3 expression on cell function, we assessed the apoptotic cell marker, annexin V, and necrotic cell markers, PI and 7-AAD, using flow cytometry. As shown in Fig. 7D, shRNA against LPCAT3 resulted in almost a 2-fold increase in annexin V staining, compared with controls, in HEK293 cells. The overall level of apoptosis in these cells was still below 10%. PI and 7-ADD staining were unaffected (data not shown). These data suggest that limiting LPCAT3 expression induced apoptosis-specific cell death in a subpopulation of HEK293 cells but did not induce population-wide DNA damage or decrease membrane integrity. However, transfection with LPCAT3 shRNA had a striking effect on cell morphology. There were far fewer lamellipodia and less cell spreading compared with controls (**Fig. 8**).

DISCUSSION

This study extends our previous characterization of the yeast lysophospholipid acyltransferase, Lpt1, to the human genome. The homologous LPCAT3 was chosen based on its conservation of the ER retention signal and previous studies where LPCAT3-specific siRNA reduced LPCAT activity in human Huh7 cells by 90% (19) and mouse B16

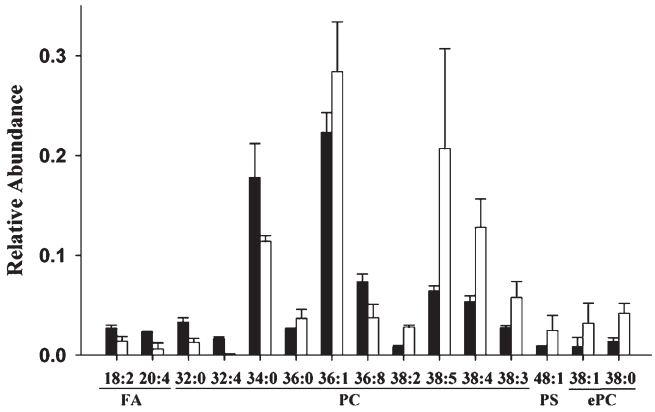

Fig. 6. Effect of reducing LPCAT3 expression on phospholipid species. HEK293 cells were transfected with a control, nonsilencing (NS) shRNA plasmid (dark bars) or a shRNA plasmid targeting LPCAT3 expression (light bars). After 24 h, cells were removed from the dish and analyzed as described in Fig. 5. Of the *m/z* values analyzed, all that statistically differed between NS and LPCAT3 are shown; $P < 0.05$. Standard error bars are shown. LPCAT, lysophosphatidylcholine acyltransferase.

melanoma cells (18) by 50%. This preliminary evidence suggests that LPCAT3 is responsible for a large proportion of LPCAT activity in vivo in at least some cell types. Ours is the first report of baculovirus-mediated expression of LPCAT3 in Sf9 insect cells conferring esterification of lysoPC, lysoPE, and lysoPS in vitro. The use of lysoPE as a substrate differs from one earlier report (19) but confirms the findings of others (18, 30, 33). Since 1-alkyl lysoPC and lysoPA were not used as substrates, LPCAT3 does not seem to have a direct role in plasmalogen or de novo phospholipid synthesis. We maintained the use of the LPCAT3 nomenclature based on established precedent, even though the enzyme's substrate specificity includes lysoPL species with amine head groups.

The observation that human LPCAT3 used unsaturated acyl-CoA species in vitro with higher capacity (i.e., apparent V_{max}) than a saturated acyl-CoA is similar to that in other studies. However, our studies show generally greater activity with the monounsaturated oleoyl-CoA than the polyunsaturated species. This is in contrast with a recently published mass spectrometry–based assay of LPCAT3 expressed in *ale1Δ* (*lpt1Δ*) yeast which detected a profound preference for linoleoyl-CoA and arachidonyl-CoA with little utilization of 18:1 acyl-CoA (33). Expression of human LPCAT3 in HEK293 cells also found a preference for arachidonyl-CoA compared with oleoyl-CoA, along with a fairly robust activity with stearoyl-CoA; a V_{max} 1:5 of that of oleoyl-CoA (19). The ratio in our study was 1:15.

Consistent with these differences, the effects on phospholipid species as measured using ESI-MS were different compared with other studies. The use of LPCAT3 targeted siRNA in mouse B16 melanoma cells detected a 20% reduction in 16:0, 18:2 and 16:0, 20:4 species of PC (18). [^{14}C]Arachidonyl-CoA pulse labeling of HeLa treated with LPCAT3 siRNA identified decreased incorporation into PC, PE, and PS (30). Our experiment of reducing LPCAT3

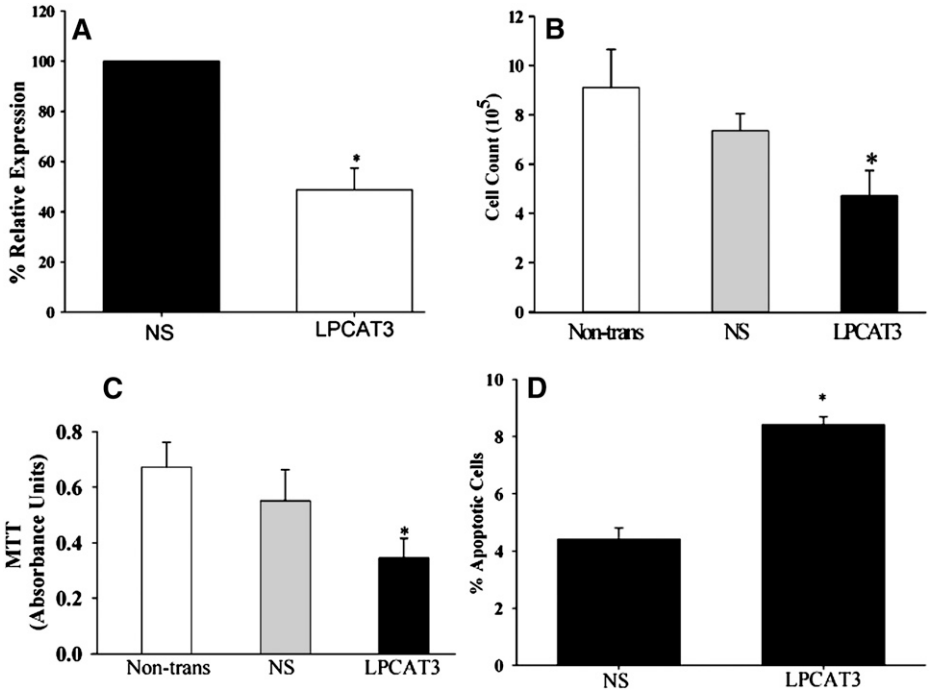

Fig. 7. Effect of LPCAT-targeted shRNA on HEK293 cells. HEK293 cells were either nontransfected (non-trans.) or transfected and cultured as described in Fig. 6. Cells were harvested and analyzed as follows. A: RT-PCR with LPCAT3 specific primers; B: Flow cytometry to determine cell number; C: MTT staining to measure electron transport through complex I; and D: Annexin V staining to measure apoptosis. Asterisk indicates statistically significant difference with NS-control ($P < 0.05$). LPCAT, lysophosphatidylcholine acyltransferase. Standard error bars are shown.

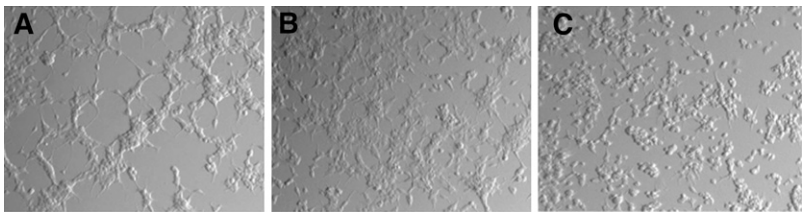

Fig. 8. Effect of LPCAT3-targeted shRNA on cell morphology. HEK293 cells were transfected or not as described in Fig. 6. A: Nontransfected. B: Nonsilencing shRNA. C: LPCAT3 shRNA. After 24 h., cells were visualized by phase-contrast microscopy (25× magnification). A representative field of view is shown for each. LPCAT, lysophosphatidylcholine acyltransferase.

expression in HEK293 cells resulted in an increase in polyunsaturated acyl chains in PC. This might be considered an anomaly if not for the concomitant decrease in polyunsatured chains that was observed when LPCAT3 was over expressed in Sf9 cells. Perhaps the contrasting results are due to a combination of different methodologies and cell types. These discrepancies are interesting to compare with LPCAT activity in rat liver microsomes, which preferentially utilize oleoyl-CoA and arachidonyl-CoA (34).

Particularly unique to these studies is the observed increase in apoptosis with reduction of LPCAT3 expression via shRNA. This is consistent with a recent finding that lysoPC is the "death effector" in lipoapoptosis in cultured hepatocytes (35). While lysoPC levels were below the sensitivity of the ESI-MS methods employed, these will likely increase upon the limitation of LPCAT3 expression. The reduction in lamellipodia is also in line with previous findings that showed RNAi driven reduction of LPCAT3 (C3F) expression in HeLa cells resulting in Golgi fragmentation (36). Pharmacological inhibition of LPCAT activity resulted in Golgi tubulation in rat clone 9 hepatocytes (37). Also, disruption of the Golgi by Brefeldin A has been shown to limit lamellipodia in Swiss 3T3 fibroblasts (38). Taken together, these data suggest that reduced LPCAT3 activity disrupts Golgi structure, limiting plasma membrane extension and cell proliferation.

Also novel was the finding that acyl-CoA utilization by LPCAT3 displays cooperativity. One possible explanation is that at low substrate concentrations, diffusion rates into membranes are a limiting factor, and accordingly, activity is disproportionately low. However, there are precedents for two members of the MBOAT gene family showing substrate binding cooperativity. Purified *Brassica napus* acyl-CoA diacylglycerol acyltransferase 1 (DGAT1) has shown cooperative oleoyl-CoA binding which coincides with protein forming homotetramers (39). Human acyl-CoA cholesterol acyl-CoA transferase 1 (ACAT1) has been clearly shown to bind cholesterol in a cooperative fashion (40) and form homotetramers (41). Whether LPCAT3 forms multimers remains to be determined.

In summary, LPCAT3 expression in tissue culture increased the abundance of phospholipids with relatively more saturated acyl chains, whereas limiting LPCAT3 expression increased the abundance of phospholipids with more unsaturated acyl chains. This is consistent with the kinetic data if cellular acyl-CoA concentrations are 5 μM or lower. Kinetic analysis of LPCAT3 also detected a novel sigmoidal relationship between acyl-CoA concentration and activity consistent with cooperativity. While LPCAT3 expression has been reduced in tissue culture by other investigators, this study is the first to show a morphological phenotype and increased occurrence of apoptosis.

The authors thank David Schultz at the Wistar Institute Protein Expression Core Facility for excellent technical assistance in baculovirus and Sf9 cell propagation and infection.

REFERENCES

1. Lands, W. E. 1960. Metabolism of glycerolipids. 2. The enzymatic acylation of lysolecithin. *J. Biol. Chem.* **235:** 2233–2237.
2. Holte, L. L., F. Separovic, and K. Gawrisch. 1996. Nuclear magnetic resonance investigation of hydrocarbon chain packing in bilayers of polyunsaturated phospholipids. *Lipids.* **31(Suppl):** S199–S203.
3. Mahoney, E. M., W. A. Scott, F. R. Landsberger, A. L. Hamill, and Z. A. Cohn. 1980. Influence of fatty acyl substitution on the composition and function of macrophage membranes. *J. Biol. Chem.* **255:** 4910–4917.
4. Post, M., E. A. Schuurmans, J. J. Batenburg, and L. M. Van Golde. 1983. Mechanisms involved in the synthesis of disaturated phosphatidylcholine by alveolar type II cells isolated from adult rat lung. *Biochim. Biophys. Acta.* **750:** 68–77.
5. Xu, Y., A. Malhotra, M. Ren, and M. Schlame. 2006. The enzymatic function of tafazzin. *J. Biol. Chem.* **281:** 39217–39224.
6. Funk, C. D. 2001. Prostaglandins and leukotrienes: advances in eicosanoid biology. *Science.* **294:** 1871–1875.
7. Xu, Y. 2002. Sphingosylphosphorylcholine and lysophosphatidylcholine: G protein-coupled receptors and receptor-mediated signal transduction. *Biochim. Biophys. Acta.* **1582:** 81–88.
8. Nakanishi, H., H. Shindou, D. Hishikawa, T. Harayama, R. Ogasawara, A. Suwabe, R. Taguchi, and T. Shimizu. 2006. Cloning and characterization of mouse lung-type acyl-CoA:lysophosphatidylcholine acyltransferase 1 (LPCAT1). Expression in alveolar type II cells and possible involvement in surfactant production. *J. Biol. Chem.* **281:** 20140–20147.
9. Chen, X., B. A. Hyatt, M. L. Mucenski, R. J. Mason, and J. M. Shannon. 2006. Identification and characterization of a lysophosphatidylcholine acyltransferase in alveolar type II cells. *Proc. Natl. Acad. Sci. USA.* **103:** 11724–11729.
10. Shindou, H., D. Hishikawa, H. Nakanishi, T. Harayama, S. Ishii, R. Taguchi, and T. Shimizu. 2007. A single enzyme catalyzes both platelet-activating factor production and membrane biogenesis of inflammatory cells. Cloning and characterization of acetyl-CoA:LYSO-PAF acetyltransferase. *J. Biol. Chem.* **282:** 6532–6539.
11. Soupene, E., H. Fyrst, and F. A. Kuypers. 2008. Mammalian acyl-CoA:lysophosphatidylcholine acyltransferase enzymes. *Proc. Natl. Acad. Sci. USA.* **105:** 88–93.
12. Riekhof, W. R., J. Wu, M. A. Gijon, S. Zarini, R. C. Murphy, and D. R. Voelker. 2007. Lysophosphatidylcholine metabolism in Saccharomyces cerevisiae: the role of P-type ATPases in transport and a broad specificity acyltransferase in acylation. *J. Biol. Chem.* **282:** 36853–36861.
13. Jain, S., N. Stanford, N. Bhagwat, B. Seiler, M. Costanzo, C. Boone, and P. Oelkers. 2007. Identification of a novel lysophospholipid acyltransferase in Saccharomyces cerevisiae. *J. Biol. Chem.* **282:** 30562–30569.
14. Benghezal, M., C. Roubaty, V. Veepuri, J. Knudsen, and A. Conzelmann. 2007. SLC1 and SLC4 encode partially redundant acyl-coenzyme A 1-acylglycerol-3-phosphate O-acyltransferases of budding yeast. *J. Biol. Chem.* **282:** 30845–30855.
15. Tamaki, H., A. Shimada, Y. Ito, M. Ohya, J. Takase, M. Miyashita, H. Miyagawa, H. Nozaki, R. Nakayama, and H. Kumagai. 2007. LPT1

encodes a membrane-bound O-acyltransferase involved in the acylation of lysophospholipids in the yeast Saccharomyces cerevisiae. *J. Biol. Chem.* **282:** 34288–34298.
16. Chen, Q., M. Kazachkov, Z. Zheng, and J. Zou. 2007. The yeast acylglycerol acyltransferase LCA1 is a key component of Lands cycle for phosphatidylcholine turnover. *FEBS Lett.* **581:** 5511–5516.
17. Hofmann, K. 2000. A superfamily of membrane-bound O-acyltransferases with implications for Wnt signaling. *Trends Biochem. Sci.* **25:** 111–112.
18. Hishikawa, D., H. Shindou, S. Kobayashi, H. Nakanishi, R. Taguchi, and T. Shimizu. 2008. Discovery of a lysophospholipid acyltransferase family essential for membrane asymmetry and diversity. *Proc. Natl. Acad. Sci. USA.* **105:** 2830–2835.
19. Zhao, Y., Y. Q. Chen, T. M. Bonacci, D. S. Bredt, S. Li, W. R. Bensch, D. E. Moller, M. Kowala, R. J. Konrad, and G. Cao. 2008. Identification and characterization of a major liver lysophosphatidylcholine acyltransferase. *J. Biol. Chem.* **283:** 8258–8265.
20. Labarga, A., F. Valentin, M. Anderson, and R. Lopez. 2007. Web services at the European Bioinformatics Institute. *Nucleic Acids Res.* (Web Server issue.) **35:** W6–11.
21. Krogh, A., B. Larsson, G. von Heijne, and E. L. Sonnhammer. 2001. Predicting transmembrane protein topology with a hidden Markov model: application to complete genomes. *J. Mol. Biol.* **305:** 567–580.
22. Yen, C. L., S. J. Stone, S. Cases, P. Zhou, and R. V. Farese, Jr. 2002. Identification of a gene encoding MGAT1, a monoacylglycerol acyltransferase. *Proc. Natl. Acad. Sci. USA.* **99:** 8512–8517.
23. Bligh, E. G., and W. J. Dyer. 1959. A rapid method of total lipid extraction and purification. *Can. J. Biochem. Physiol.* **37:** 911–917.
24. Taguchi, R., J. Hayakawa, Y. Takeuchi, and M. Ishida. 2000. Two-dimensional analysis of phospholipids by capillary liquid chromatography/electrospray ionization mass spectrometry. *J. Mass Spectrom.* **35:** 953–966.
25. Cummings, B. S., and R. G. Schnellmann. 2002. Cisplatin-induced renal cell apoptosis: caspase 3-dependent and -independent pathways. *J. Pharmacol. Exp. Ther.* **302:** 8–17.
26. Cummings, B. S., G. R. Kinsey, L. J. Bolchoz, and R. G. Schnellmann. 2004. Identification of caspase-independent apoptosis in epithelial and cancer cells. *J. Pharmacol. Exp. Ther.* **310:** 126–134.
27. Altschul, S. F., W. Gish, W. Miller, E. W. Myers, and D. J. Lipman. 1990. Basic local alignment search tool. *J. Mol. Biol.* **215:** 403–410.
28. Nilsson, T., M. Jackson, and P. A. Peterson. 1989. Short cytoplasmic sequences serve as retention signals for transmembrane proteins in the endoplasmic reticulum. *Cell.* **58:** 707–718.
29. Kazachkov, M., Q. Chen, L. Wang, and J. Zou. 2008. Substrate preferences of a lysophosphatidylcholine acyltransferase highlight its role in phospholipid remodeling. *Lipids.* **43:** 895–902.
30. Matsuda, S., T. Inoue, H. C. Lee, N. Kono, F. Tanaka, K. Gengyo-Ando, S. Mitani, and H. Arai. 2008. Member of the membrane-bound O-acyltransferase (MBOAT) family encodes a lysophospholipid acyltransferase with broad substrate specificity. *Genes Cells.* **13:** 879–888.
31. Strausberg, R. L., E. A. Feingold, R. D. Klausner, and F. S. Collins. 1999. The mammalian gene collection. *Science.* **286:** 455–457.
32. Cheng, D., C. C. Chang, X. Qu, and T. Y. Chang. 1995. Activation of acyl-coenzyme A:cholesterol acyltransferase by cholesterol or by oxysterol in a cell-free system. *J. Biol. Chem.* **270:** 685–695.
33. Gijon, M. A., W. R. Riekhof, S. Zarini, R. C. Murphy, and D. R. Voelker. 2008. Lysophospholipid acyltransferases and arachidonate recycling in human neutrophils. *J. Biol. Chem.* **283:** 30235–30245.
34. Yamashita, S., K. Hosaka, Y. Miki, and S. Numa. 1981. Glycerolipid acyltransferases from rat liver: 1-acylglycerophosphate acyltransferase, 1-acylglycerophosphorylcholine acyltransferase, and diacylglycerol acyltransferase. *Methods Enzymol.* **71 (Pt C):** 528–536.
35. Han, M. S., S. Y. Park, K. Shinzawa, S. Kim, K. W. Chung, J. H. Lee, C. H. Kwon, K. W. Lee, J. H. Lee, C. K. Park, et al. 2008. Lysophosphatidylcholine as a death effector in the lipoapoptosis of hepatocytes. *J. Lipid Res.* **49:** 84–97.
36. Hodges, E., J. S. Redelius, W. Wu, and C. Hoog. 2005. Accelerated discovery of novel protein function in cultured human cells. *Mol. Cell. Proteomics.* **4:** 1319–1327.
37. Drecktrah, D., K. Chambers, E. L. Racoosin, E. B. Cluett, A. Gucwa, B. Jackson, and W. J. Brown. 2003. Inhibition of a Golgi complex lysophospholipid acyltransferase induces membrane tubule formation and retrograde trafficking. *Mol. Biol. Cell.* **14:** 3459–3469.
38. Bershadsky, A. D., and A. H. Futerman. 1994. Disruption of the Golgi apparatus by brefeldin A blocks cell polarization and inhibits directed cell migration. *Proc. Natl. Acad. Sci. USA.* **91:** 5686–5689.
39. Weselake, R. J., M. Madhavji, S. J. Szarka, N. A. Patterson, W. B. Wiehler, C. L. Nykiforuk, T. L. Burton, P. S. Boora, S. C. Mosimann, N. A. Foroud, et al. 2006. Acyl-CoA-binding and self-associating properties of a recombinant 13.3 kDa N-terminal fragment of diacylglycerol acyltransferase-1 from oilseed rape. *BMC Biochem.* **7:** 24.
40. Chang, C. C., C. Y. Lee, E. T. Chang, J. C. Cruz, M. C. Levesque, and T. Y. Chang. 1998. Recombinant acyl-CoA:cholesterol acyltransferase-1 (ACAT-1) purified to essential homogeneity utilizes cholesterol in mixed micelles or in vesicles in a highly cooperative manner. *J. Biol. Chem.* **273:** 35132–35141.
41. Yu, C., Y. Zhang, X. Lu, J. Chen, C. C. Chang, and T. Y. Chang. 2002. Role of the N-terminal hydrophilic domain of acyl-coenzyme A:cholesterol acyltransferase 1 on the enzyme's quaternary structure and catalytic efficiency. *Biochemistry.* **41:** 3762–3769.